Inhibition of KIR2.1 decreases pulmonary artery smooth muscle cell proliferation and migration

NAN CAO[1-3*], NIGALA AIKEREMU[1,3*], WEN-YAN SHI[1,3*], XUE-CHUN TANG[1,3,4], RUI-JUAN GAO[1,3,5], LIANG-JING-YUAN KONG[1,3], JING-RONG ZHANG[1,3], WEN-JUAN QIN[6], AI-MEI ZHANG[7], KE-TAO MA[1,3], LI LI[8] and JUN-QIANG SI[1,3,9,10]

[1]Department of Physiology, Shihezi University Medical College, Shihezi, Xinjiang 832002; [2]Department of Physiology and Pathophysiology, Kangda College of Nanjing Medical University, Lianyungang, Jiangsu 222061; [3]Key Laboratory of Xinjiang Endemic and Ethnic Diseases, Shihezi University Medical College; Departments of [4]Burns, [5]Radiology, [6]Ultrasound and [7]Cardiology, The First Affiliated Hospital of Shihezi University, Shihezi, Xinjiang 832002; [8]Department of Physiology, Jiaxing University Medical College, Jiaxing, Zhejiang 314001; [9]Department of Physiology, Wuhan University School of Basic Medical Sciences, Wuhan, Hubei 430072; [10]Department of Physiology, Huazhong University of Science and Technology of Basic Medical Sciences, Wuhan, Hubei 430070, P.R. China

Received April 5, 2022; Accepted June 28, 2022

DOI: 10.3892/ijmm.2022.5175

Abstract. The investigation of effective therapeutic drugs for pulmonary hypertension (PH) is critical. KIR2.1 plays crucial roles in regulating cell proliferation and migration, and vascular remodeling. However, researchers have not yet clearly determined whether KIR2.1 participates in the proliferation and migration of pulmonary artery smooth muscle cells (PASMCs) and its role in pulmonary vascular remodeling (PVR) also remains elusive. The present study aimed to examine whether KIR2.1 alters PASMC proliferation and migration, and participates in PVR, as well as to explore its mechanisms of action. For the *in vivo* experiment, a PH model was established by intraperitoneally injecting Sprague-Dawley rats monocrotaline (MCT). Hematoxylin and eosin staining revealed evidence of PVR in the rats with PH. Immunofluorescence staining and western blot analysis revealed increased levels of the KIR2.1, osteopontin (OPN) and proliferating cell nuclear antigen (PCNA) proteins in pulmonary blood vessels and lung tissues following exposure to MCT, and the TGF-β1/SMAD2/3 signaling pathway was activated. For the *in vitro* experiments, the KIR2.1 inhibitor, ML133, or the TGF-β1/SMAD2/3 signaling pathway blocker, SB431542, were used to pre-treat human PASMCs (HPASMCs) for 24 h, and the cells were then treated with platelet-derived growth factor (PDGF)-BB for 24 h. Scratch and Transwell assays revealed that PDGF-BB promoted cell proliferation and migration. Immunofluorescence staining and western blot analysis demonstrated that PDGF-BB upregulated OPN and PCNA expression, and activated the TGF-β1/SMAD2/3 signaling pathway. ML133 reversed the proliferation and migration induced by PDGF-BB, inhibited the expression of OPN and PCNA, inhibited the TGF-β1/SMAD2/3 signaling pathway, and reduced the proliferation and migration of HPASMCs. SB431542 pre-treatment also reduced cell proliferation and migration; however, it did not affect KIR2.1 expression. On the whole, the results of the present study demonstrate that KIR2.1 regulates the TGF-β1/SMAD2/3 signaling pathway and the expression of OPN and PCNA proteins, thereby regulating the proliferation and migration of PASMCs and participating in PVR.

Correspondence to: Professor Jun-Qiang Si, Department of Physiology, Shihezi University Medical College, 59 Beier Road, Shihezi, Xinjiang 832002, P.R. China
E-mail: sijunqiang@shzu.edu.cn

Professor Li Li, Department of Physiology, Jiaxing University Medical College, 118 Jiahang Road, Nanhu, Jiaxing, Zhejiang 314001, P.R. China
E-mail: lily7588@163.com

*Contributed equally

Key words: KIR2.1, proliferation, migration, pulmonary artery smooth muscle cell, pulmonary hypertension

Introduction

Pulmonary hypertension (PH) is a cardiopulmonary vascular disease characterized by continued increases in pulmonary arterial pressure and pulmonary vascular resistance (1). Current treatment strategies mainly focus on reducing pulmonary vascular resistance and increasing blood flow. However, these approaches are not effective for a long period of time. Therefore, the identification of a precise therapeutic target for PH is critical. The hallmark feature of PH is medial pulmonary artery hyperplasia, which is mainly caused by the abnormal proliferation and aggregation of pulmonary artery smooth muscle cells (PASMCs) (2,3). Therefore, the proliferation, migration, apoptosis and extracellular matrix deposition of PASMCs are critical targets for studying PH.

A number of growth factors are related to PH and vascular remodeling, including platelet-derived growth factor (PDGF)-BB and transforming growth factor (TGF)-β (4). The inhibition of the PDGF receptor has been shown to increase the survival rate of rats with monocrotaline (MCT)-induced PH (5,6). The TGF-β superfamily contains a large number of cytokine growth factors that control numerous cellular functions, including proliferation, migration, differentiation, and extracellular matrix secretion and deposition (4). It has been reported that PDGF-BB activates the TGF-β1/SMAD2/3 signaling pathway, and induces the growth and proliferation of rat PASMCs (7). The TGF-β1/SMAD pathway is activated in animals with MCT and hypoxia-induced PH (8-10) and in patients with PH (11). The activation of the TGF-β1/SMAD2/3 signaling pathway is one of the factors contributing to the occurrence and development of PH.

Inwardly rectifying K^+ channel (KIR)2.1 encoded by the *KCNJ2* gene is a member of the classical inwardly rectifying K^+ channel family (KIR2 subfamily). In previous research, KIR2.1 was considered the main component of the inward rectifying potassium current of the heart and an essential component of the stable resting membrane potential of cardiomyocytes (12). However, KIR2.1 is related to cell proliferation and migration (13-17) and vascular remodeling (18). According to previous studies, KIR2.1 is expressed in isolated rat basilar artery, coronary artery, mesenteric artery smooth muscle cells (19), renal arteriole smooth muscle cells (20) and PASMCs (21). KIR2.1 gene knockout significantly inhibits the proliferation and migration of rat vascular smooth muscle cells (VSMCs) stimulated by PDGF-BB (22). However, researchers have not yet determined whether KIR2.1 participates in the proliferation and migration of PASMCs.

Therefore, the present study aimed to examine the effects of KIR2.1 inhibition on the proliferation and migration of PASMCs induced by PDGF-BB. In addition, the present study examined whether KIR2.1 regulates the TGF-β1/Smad2/3 signaling pathway by maintaining the depolarized membrane potential of the cell membrane, and whether it regulates the proliferation and migration of PASMCs.

Materials and methods

Animal model and treatment strategy. A total of 12 Sprague-Dawley (SD) rats (8-10 weeks old, weighing 200-250 g) were used in the experiments. The rats were purchased from Beijing Vital River Experimental Animal Co., Ltd. (license no. SCXK Beijing 2016-0006). The animals were maintained in environmentally controlled conditions (adequate cage size; free access to food and water; temperature, 22±2˚C; humidity, 50-55%) on a 12-h light/12-h dark cycle. All procedures involving animals were performed in accordance with ethical standards and approved by the Institutional Animal Care and Use Committee of the Affiliated Hospital of Shihezi University School of Medicine (approval no. A 2020-165-01). Applicable guidelines were followed in accordance with the 'Guide for the Care and Use' published by the American Physiological Society (23).

A total of 12 rats were randomly and equally divided into two groups as follows: The control (CON) group and MCT group [60 mg/kg MCT (24-26) administered by intraperitoneal (i.p.) injection on the first day; Sigma-Aldrich; Merck KGaA].

Doppler echocardiography measurements. The Doppler echo parameter, pulmonary artery acceleration time (PAAT) is considered an echocardiographic indicator of PH (27). PAAT is the time interval between the onset of systolic pulmonary arterial flow and peak flow velocity. Previous studies have demonstrated that PAAT is inversely proportional to pulmonary vascular resistance (28-30). If the pulmonary vascular resistance increases, the pulmonary artery pressure also increases. Doppler echocardiography was used to assess PH on the 28th day following model establishment in the SD rats. A transthoracic closed-chest echocardiography was performed using a Vivid E9 ultrasound system equipped with a 12-MHz transducer (GE Healthcare; Cytiva). The rats were anesthetized by administering an i.p. injection of 3% sodium pentobarbital (40 mg/kg). PAAT was measured near the pulmonary valve on the left side of the chest. EchoPAC™ BT11 software (v.6.5; GE Healthcare; Cytiva) was used to analyze the data.

Right ventricular hypertrophy measurement. For the measurement of right ventricular hypertrophy, the rats were euthanized by an i.p. injection of 3% sodium pentobarbital (100 mg/kg) combined with CO_2 anesthesia at a displacement of 70% vol/min. The heart tissue was collected and weighed to evaluate the right ventricular hypertrophy index (RVHI). The atrium and external blood vessels were separated from the isolated heart in 0.9% normal saline. The weights of both the right ventricle (RV) and left ventricle (LV) plus septum (S) were recorded. The RVHI was calculated using the formula: [RV/(LV + S)].

Histopathological examination of lung tissue. Lung tissues were harvested, fixed in 4% paraformaldehyde (Boster Co., Ltd.), dehydrated, cleared, waxed, embedded, sectioned, patched and cut into slices (4-μm-thick). Hematoxylin and eosin (H&E) staining or Masson's trichome staining (Beijing Solarbio Biotechnology Co., Ltd.) were used to evaluate the pulmonary artery morphology. Lung tissues were observed and photographed using a digital camera (BX51; Olympus Corporation). Image-Pro Plus v.6.0 software (Media Cybernetics, Inc.) was used for the quantitative analysis. Pulmonary vascular remodeling (PVR) was evaluated by calculating the percentage of the thickness of the vessel wall (WT%) and the percentage of the vessel wall area (WA%): WT%=[2x (blood vessel outer diameter-blood vessel inner diameter)]/(blood vessel outer diameter) x100%; WA%=(total area of blood vessel-blood vessel internal area)/total area of blood vessel x100% (31). Two professional pathologists randomly selected 20 different non-overlapping fields from each section and analyzed PVR and lung fibrosis with Image-Pro Plus v.6.0 software (Media Cybernetics, Inc.). The pulmonary fibrosis index was analyzed by calculating the ratio of the total area of collagen to the total area of connective tissue in each field of view, as previously described (32).

Cell culture and treatment. Human PASMCs (HPASMCs) (Shanghai iCell Bioscience Inc.) were cultured in high-glucose DMEM (Gibco; Thermo Fisher Scientific, Inc.) supplemented

with 10% fetal bovine serum (FBS) and 1% penicillin-streptomycin (Gibco; Thermo Fisher Scientific, Inc.). The cells were incubated at 37˚C for 24 h in a humidified 5% CO_2 atmosphere.

For the cell treatments, the cells were first pre-treated with the KIR2.1 pathway blocker, ML133 (20 μM, ApexBio) (14,17,33), or the TGF-β1/SMAD signaling pathway blocker, SB431542 (10 μM, ApexBio), for 24 h and were then treated with PDGF-BB (25 ng/ml, PeproTech, Inc.) (34-36) for 24 h. Cells in the control group were not treated. The experiment was repeated six times (n=6).

Cell scratch assay. HPASMCs in the logarithmic growth phase were plated as monolayers on six-well plates and cultured at 37˚C with 5% CO_2 until the cell density reached 80%. A cell-free band was uniformly generated at the center of each well using a 1-ml pipet tip. The cells were washed twice with PBS and then incubated with 2 ml 2% DMEM/F12 low-serum medium and pretreated with 0 μM ML133 for 24 h, then treated with 25 ng/ml PDGF-BB for 24 h. Images were recorded and assessed at 0 and 24 h using an Olympus inverted microscope (Olympus Corporation). The migration distance was estimated using ImageJ v1.8.0 software (National Institutes of Health). The cell migration rate (%)=[(0 h average scratch area-24 h average scratch area)/0 h average scratch area] x100% (37-39).

Transwell assay. The Transwell™ chamber (Corning, Inc.) was placed in a 24-well culture plate. Subsequently, 200 μl of the cell suspension (cell density of 10^4 cells/ml) were inoculated into the upper chamber. Complete DMEM/F12 containing 10% FBS (600 μl) was then added to the lower chamber. 20 μM ML133 was added for 24 h after the cells adhered to the well, then treated with 25 ng/ml PDGF-BB for 24 h. Following the intervention, the cells were cultured with fresh medium at 37˚C in a humidified atmosphere containing 5% CO_2 for 24 h. Subsequently, the cells below the membrane were fixed with 4% paraformaldehyde for 10 min at room temperature and stained with 0.1% crystal violet for 30 min at room temperature. A cotton swab was used to gently remove the cells from the upper surface of the chamber. Following observation with a light microscope and imaging with a digital camera (BX51, Olympus Corporation), five different fields of view were randomly selected; the cells that invaded the submembrane surface were counted, and the number of invaded cells reflected the strength of the invasive ability of the HPASMCs (37-39).

Immunofluorescence staining. The paraffin-embedded tissue sections were dewaxed, and antigen retrieval was performed. The cells were seeded on six-well glass slides for fixation. Triton X (0.3%) was used to permeabilize the membrane. The cells were then incubated overnight at 4˚C with the following antibodies: Anti-KIR2.1 (1:100 dilution, cat. no. ab109750), anti-osteopontin (OPN; 1:500 dilution, cat. no. ab8448), anti-proliferating cell nuclear antigen (PCNA; 1:200 dilution, cat. no. ab29) and anti-α-smooth muscle actin (α-SMA; 1: 500; cat. no. ab124964) (all from Abcam). The following day, the cells were incubated with FITC-labeled goat anti-rabbit IgG (1:100; cat. no. ZF-0311) or TRITC-labeled anti-mouse IgG (1:100; ZF-0313) (Beijing Zhongshan Jinqiao Biotechnology Co., Ltd.) antibodies in a dark box at 37˚C for 2 h. The nuclei were stained with DAPI (1:1,000, D9542; Sigma-Aldrich; Merck KGaA) at 37˚C in a dark box for 20 min. The cells were observed and photographed under a fluorescence inverted microscope (LSM710; Carl Zeiss AG). Proteins were semi-quantitatively analyzed using Image-Pro Plus 6.0 software (National Institutes of Health).

Western blot analysis. Total protein was extracted from HPASMC suspensions or pulmonary vascular tissue homogenates from SD rats with RIPA Lysis Buffer (Thermo Fisher Scientific, Inc.) in western blot analysis. The BCA protein determination method was used to determine the protein concentration. Proteins aliquots (40 μg/lane) were separated using standard sodium lauryl sulfate-polyacrylamide gel electrophoresis (SDS-PAGE, (8-10% gel)) and transferred to 0.45 μm nitrocellulose membranes (Invitrogen; Thermo Fisher Scientific, Inc.). The membranes were incubated overnight at 4˚C with the following primary antibodies: Anti-GAPDH (1:10,000 dilution, cat. no. ab8245), anti-KIR2.1 (1:1,000 dilution, cat. no. ab109750), anti-TGF-β1 (1:1,000 dilution, cat. no. ab92486), anti-SMAD2 (1:1,000 dilution, cat. no. ab40855), anti-SMAD3 (1:1,000 dilution, cat. no. ab40854), anti-phosphorylated (p-)SMAD2 (1:1,000 dilution, cat. no. ab188334), anti-p-SMAD3 (1:1,000 dilution, cat. no. ab52903), anti-OPN (1:1,000 dilution, cat. no. ab8448) and anti-PCNA (1:1,000 dilution, cat. no. ab29) (all from Abcam). Subsequently, the membranes were incubated with HRP-labeled anti-mouse IgG (1:20,000 dilution; cat. no. ZB-2305) or anti-rabbit IgG (1:10,000 dilution; cat. no. ZB-5301; Beijing Zhongshan Jinqiao Biotechnology Co., Ltd.) at room temperature for 2 h. Luminescence reagents were obtained from the SuperSignal™ West Pico luminescence substrate kit (Thermo Fisher Scientific, Inc.) and incubated with the membranes. Protein bands were quantified using ImageJ v1.8.0 software (National Institutes of Health).

Statistical analysis. The statistical software packages SPSS 21.0 and GraphPad Prism 8.0 were used to analyze the experimental results. All data are presented as the mean ± standard deviations (means ± SD). The Kolmogorov-Smirnov test was used for each set of data and the data were found to be normally distributed. Differences between two groups were analyzed using unpaired t-tests. Differences in data from more than two groups were analyzed using one-way analysis of variance (ANOVA), followed by Tukey's multiple comparisons test. A value of $P<0.05$ was considered to indicate a statistically significant difference.

Results

Right ventricular remodeling and PVR in rats with PH. The echocardiogram of the blood flow in the pulmonary artery was detected using the Doppler ultrasonic diagnostic instrument. Compared with the CON group (Fig. 1A), the MCT group exhibited a midsystolic notch, with the peak shifting forward, and the PAAT value was decreased ($P<0.01$, n=6; Fig. 1B). The RVHI% of the rats in the MCT group was significantly higher than that in the CON group ($P<0.01$, n=6; Fig. 1C).

H&E staining was performed to observe the structural differences between the small pulmonary arteries (diameter,

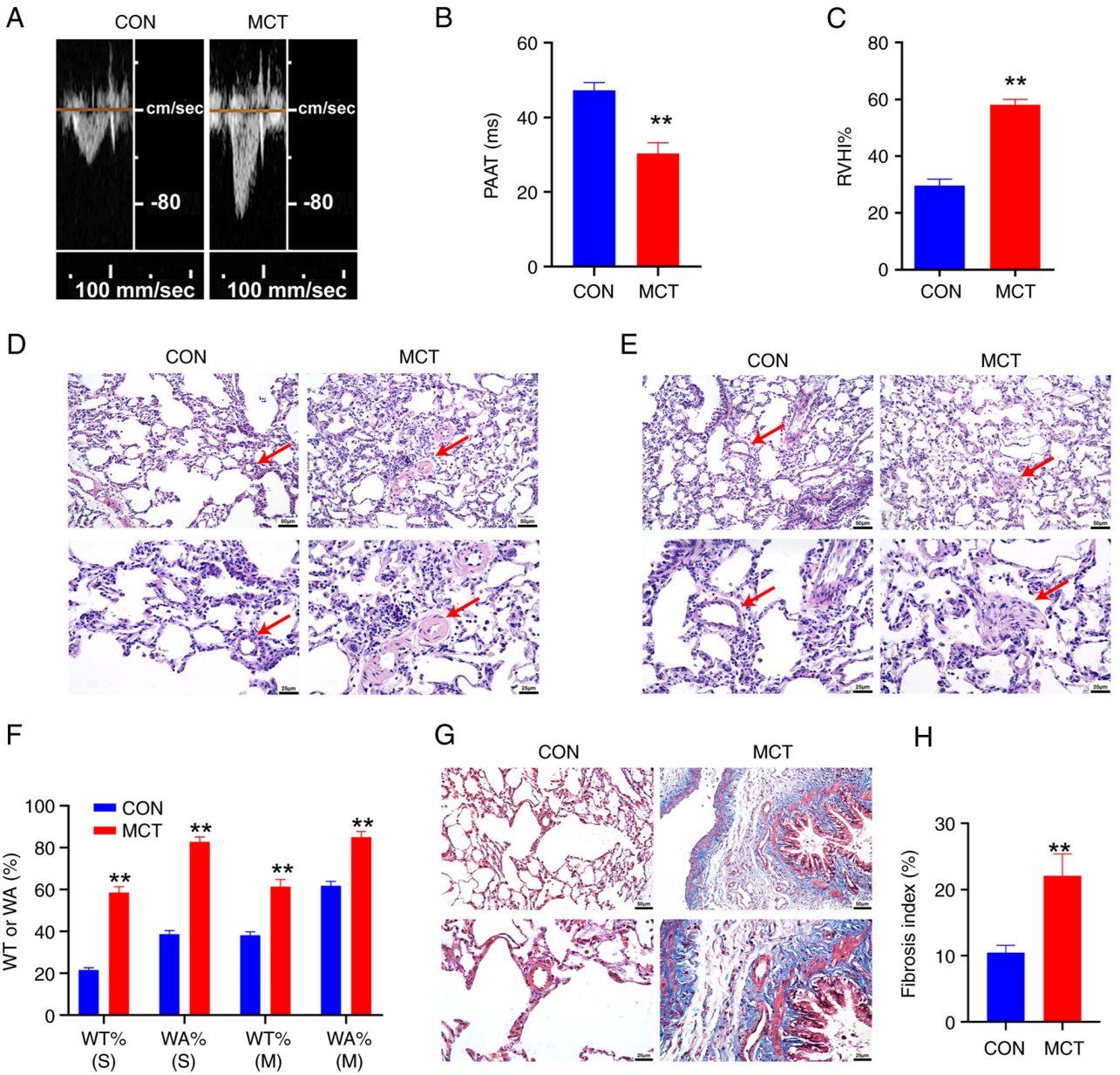

Figure 1. Right ventricular remodeling and pulmonary artery remodeling in pulmonary hypertension. (A) The pulmonary hemodynamic spectrum. (B) Comparison of PAAT. (C) Comparison of RVHI%. (D) H&E staining of the small pulmonary artery. (E) H&E staining of the middle pulmonary artery; scale bars, 50 μm (top panels) and 25 μm (bottom panels). The red arrows indicate the pulmonary artery. (F) Statistical analysis of the WT% and WA% of pulmonary arteries; scale bar, 50 or 25 μm. (G) Masson's trichrome staining of lung tissue. (H) Analysis of the fibrotic index of pulmonary vascular tissue; scale bar=50 or 25 μm. WT% (S), WT% of the small pulmonary artery; WA% (S), WA% of the small pulmonary artery; WT% (M), WT% of the middle pulmonary artery; WA% (m), WA% of the middle pulmonary artery. **P<0.01, MCT vs. CON (n=6, data were analyzed using a t-test). PAAT, pulmonary artery acceleration time; RVHI%, right ventricular hypertrophy index percentage; WT%, percentage of the thickness of the vessel wall; WA%, percentage of the vessel wall area; MCT, monocrotaline; CON, control.

15-50 μm) (Fig. 1D) and the middle pulmonary arteries (diameter, 50-150 μm) (Fig. 1E). The pulmonary artery cells in the CON group were evenly distributed, continuous and structurally intact, while the pulmonary artery cells in the MCT group exhibited a disordered arrangement, the area of the lumen was reduced, and the thickness of the tube wall was significantly increased. The pulmonary artery WT% and WA% of the MCT group were significantly higher than that of the CON group (P<0.01, n=6; Fig. 1F).

Masson's trichrome staining was used to observe collagen deposition and lung fibrosis (Fig. 1G). The analysis revealed evident collagen deposition in the pulmonary blood vessels and lung tissues of the MCT group of rats (P<0.01, Fig. 1H). The lung tissue was evidently fibrotic.

Expression of KIR2.1, OPN, PCNA and TGF-β1/SMAD2/3 signaling pathway proteins in pulmonary blood vessels and lung tissues of rats with PH. Immunohistochemistry and immunofluorescence staining were performed to detect changes in the expression of KIR2.1 (Fig. 2A and B), the migration-related protein, OPN (Fig. 2A and C), and the proliferation-related protein, PCNA (Fig. 2A and D), in rat lung tissue. The KIR2.1, OPN and PCNA proteins were widely expressed in lung tissues and pulmonary blood vessels.

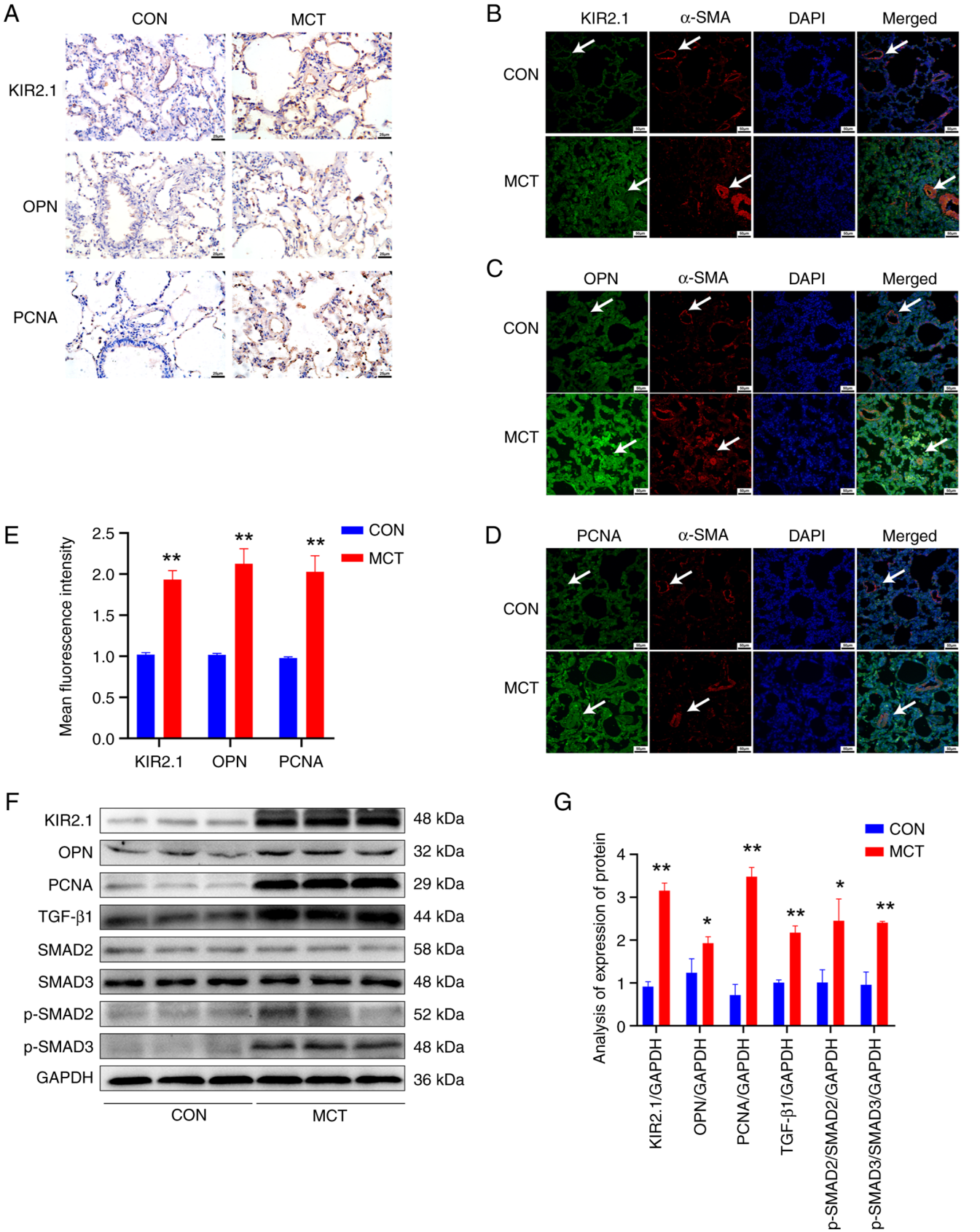

Figure 2. Expression of KIR2.1, OPN, PCNA and TGF-β1/SMAD2/3 signaling pathway proteins in pulmonary vessels and lung tissues of rats with pulmonary hypertension. (A) Immunohistochemical staining for KIR2.1, OPN and PCNA; scale bar, 25 μm. (B) Immunofluorescence staining for α-SMA and KIR2.1; (C) Immunofluorescence staining for α-SMA and OPN. (D) Immunofluorescence staining for α-SMA and PCNA. Scale bars, 50 μm. The white arrows indicate the pulmonary blood vessels. (E) Analysis of the relative expression of the KIR2.1, OPN and PCNA proteins using immunofluorescence staining. (F) Representative western blots illustrating KIR2.1, OPN, PCNA, TGF-β1, SMAD2, SMAD3, p-SMAD2, p-SMAD3 and GAPDH levels. (G) Analysis of the protein levels of KIR2.1, OPN, PCNA, TGF-β1, SMAD2, p-SMAD2, SMAD3 and p-SMAD3. *P<0.05 and **P<0.01, MCT vs. CON (n=6, data were analyzed using a t-test). KIR2.1, inwardly rectifying K^{+} channel 2.1; OPN, osteopontin; PCNA, proliferating cell nuclear antigen; α-SMA, α-smooth muscle actin; MCT, monocrotaline; CON, control.

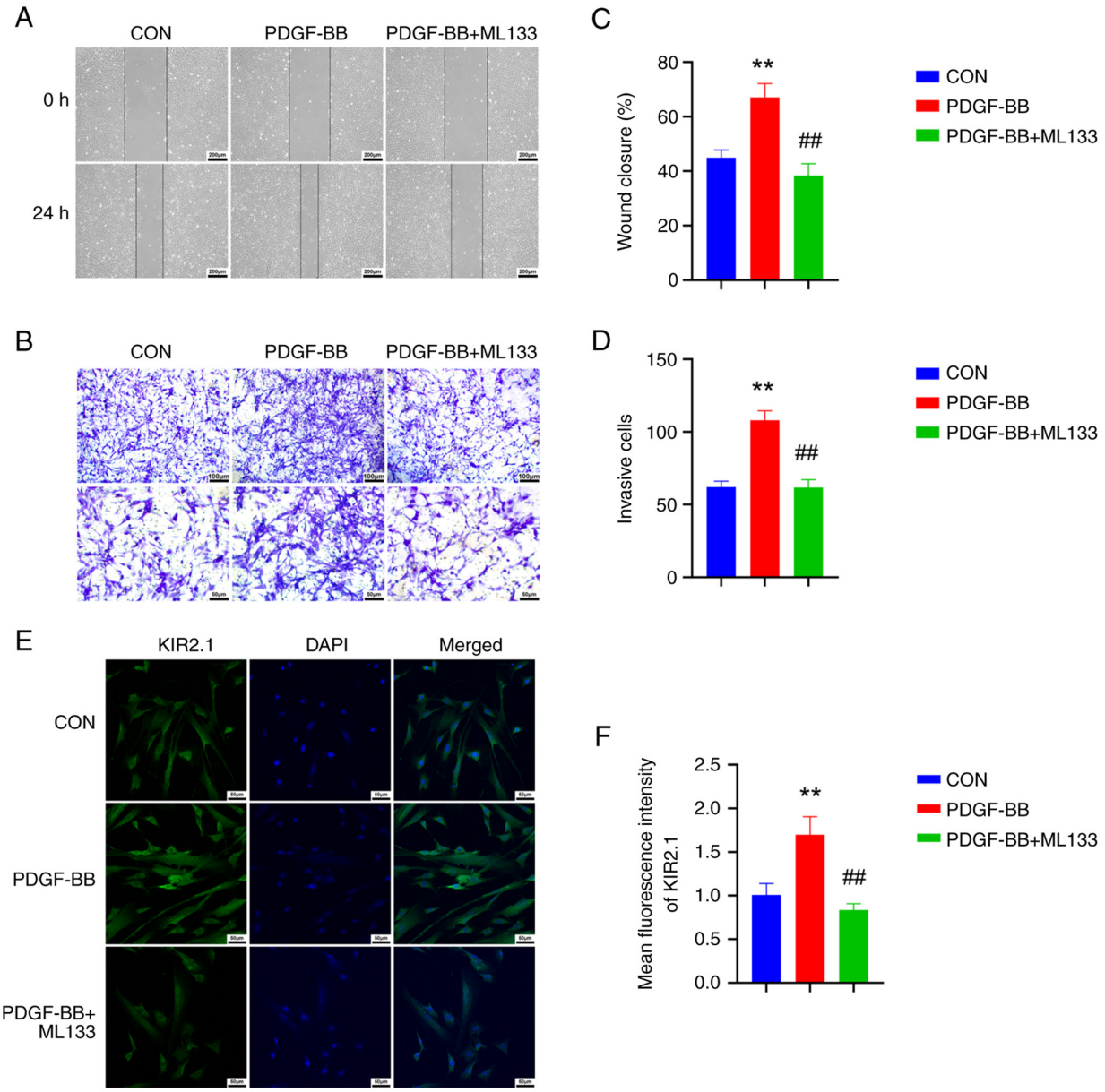

Figure 3. ML133 reverses the proliferation and migration of human pulmonary artery smooth muscle cells induced by PDGF-BB. (A) Cell scratch images; scale bar, 200 μm. (B) Crystal violet staining of the Transwell assay; scale bars, 100 μm (top panel) and 50 μm (bottom panel). (C) Quantitative analysis of the cell scratch healing rate. (D) Quantitative analysis of cell invasion. (E) Immunofluorescence staining for KIR2.1; scale bar, 50 μm. (F) Analysis of the relative expression of the KIR2.1 protein detected using immunofluorescence staining. **P<0.01, PDGF-BB vs. CON; $^{\#\#}$P<0.01, PDGF-BB + ML133 vs. PDGF-BB (n=6, data were analyzed using one-way ANOVA). PDGF-BB, platelet-derived growth factor-BB; KIR2.1, inwardly rectifying K^+ channel 2.1; CON, control.

The semi-quantitative analysis of the fluorescence intensity revealed that KIR2.1, OPN, and PCNA expression was significantly increased in the MCT group (P<0.01, n=6) compared with that in the CON group (Fig. 2E).

Western blot analysis was conducted to further detect KIR2.1, OPN and PCNA protein levels in the tissue homogenate of rat pulmonary blood vessels (Fig. 2F). The results were consistent with those of the semi-quantitative analysis of immunofluorescence staining. Significantly higher levels of the KIR2.1, OPN and PCNA proteins were detected in the MCT group compared with the CON group (P<0.01 or P<0.05, n=6; Fig. 2G). Furthermore, western blot analysis was used to assess the expression of proteins in the TGF-β1/SMAD2/3 signaling pathway in tissue homogenates of pulmonary blood vessels (Fig. 2F). Following treatment with MCT, the levels of the TGF-β1 and p-SMAD2/3 proteins were significantly increased compared with those in the CON group (P<0.01 or P<0.05, n=6; Fig. 2G).

PDGF-BB upregulates KIR2.1 protein expression, and promotes the proliferation and migration of HPASMCs, which are inhibited by ML133. HPASMCs were treated with PDGF-BB and cell proliferation, migration and changes in KIR2.1 protein expression were observed to further investigate the role of KIR2.1 in PVR. Cell proliferation and migration were analyzed using scratch and Transwell assays (Fig. 3A and C). Following stimulation with PDGF-BB, the scratch healing ability of the HPASMCs was enhanced, and the number of cells that migrated to the lower surface of the Transwell™ chamber increased (P<0.01, n=6). Moreover, cell

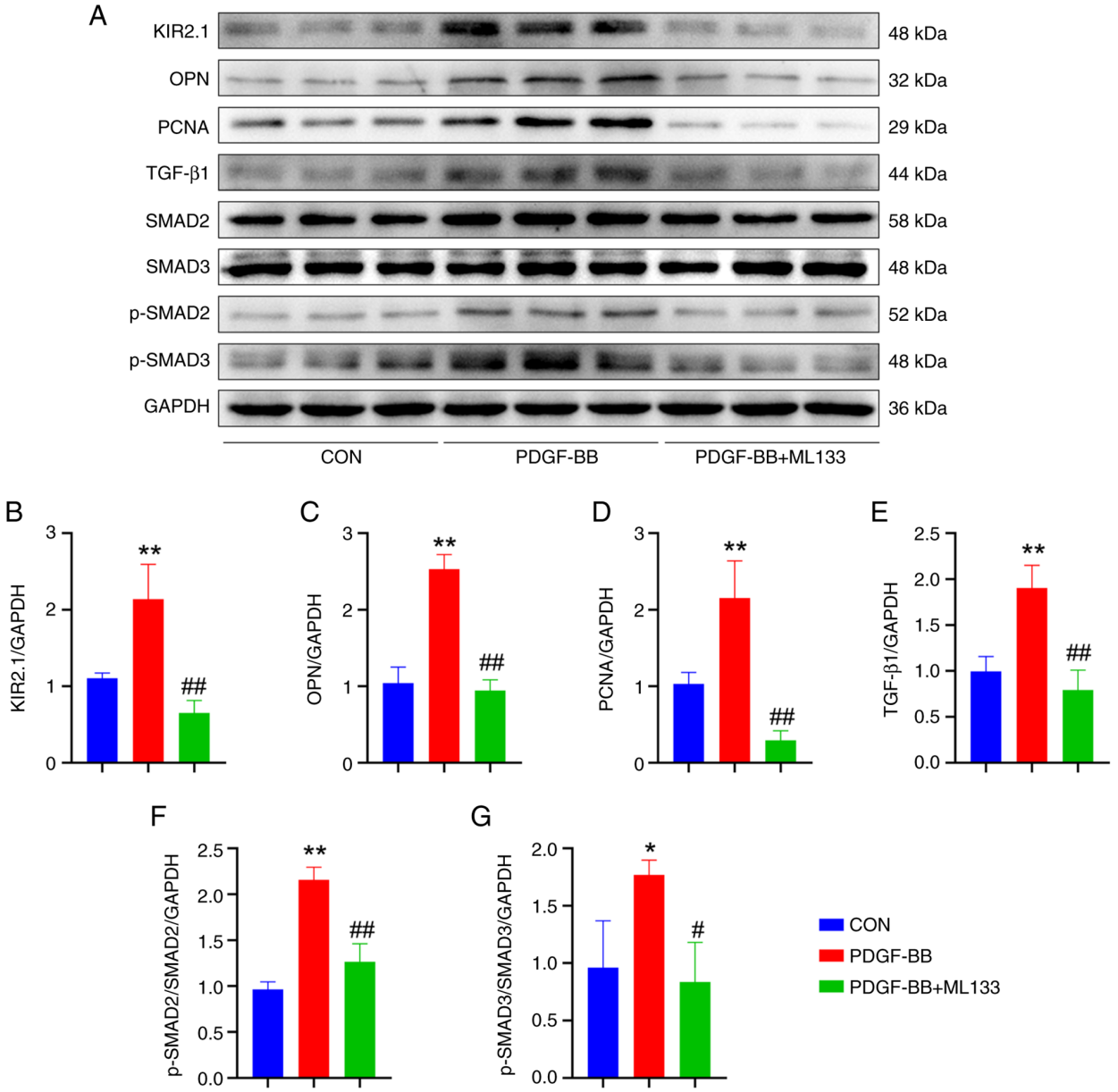

Figure 4. ML133 alters the expression of related proteins in human pulmonary artery smooth muscle cells treated with PDGF-BB. (A) Representative western blots illustrating the levels of KIR2.1, OPN, PCNA, TGF-β1, SMAD2, SMAD3, p-SMAD2, p-SMAD3 and GAPDH. (B) Analysis of KIR2.1 expression. (C) Analysis of OPN expression. (D) Analysis of PCNA expression. (E) Analysis of TGF-β1 expression. (F) Analysis of p-SMAD2 and SMAD2 levels. (G) Analysis of p-SMAD3 and SMAD3 levels. *P<0.05 and **P<0.01, PDGF-BB vs. CON; $^{\#}$P<0.05 and $^{\#\#}$P<0.01, PDGF-BB + ML133 vs. PDGF-BB (n=6, data were analyzed using one-way ANOVA). PDGF-BB, platelet-derived growth factor-BB; KIR2.1, inwardly rectifying K^{+} channel 2.1; OPN, osteopontin; PCNA, proliferating cell nuclear antigen; CON, control.

scratch healing and the number of cells migrating through the Transwell™ were reduced following pre-treatment with the KIR2.1 protein inhibitor, ML133 (P<0.01, n=6; Fig. 3B and D). The expression of the migration-related protein, OPN, and the proliferation-related protein, PCNA, in HPASMCs was detected using western blot analysis (Fig. 4A). The results were consistent with the phenotype. Following PDGF-BB intervention, the protein levels of OPN and PCNA in the HPASMCs were significantly increased (P<0.01, n=6), and OPN and the OPN and PCNA protein levels were significantly decreased in cells pre-treated with ML133 (P<0.01, n=6; Fig. 4C and D).

Immunofluorescence staining and western blot analysis were also performed to determine KIR2.1 protein expression in the HPASMCs (Figs. 3E and 4A). The results of immunofluorescence staining revealed that KIR2.1 was mainly located in the cell membrane and cytoplasm. The semi-quantitative analysis of the fluorescence intensity revealed a significantly higher protein expression of KIR2.1 in the HPASMCs stimulated with PDGF-BB than that in the CON group (P<0.01, n=6; Fig. 3E). However, KIR2.1 protein expression was decreased in the PDGF-BB + ML133 group (P<0.01, n=6; Fig. 3F). The results of western blot analysis were consistent with those from the semi-quantitative analysis of immunofluorescence staining. Following stimulation with PDGF-BB, KIR2.1 protein expression in the HPASMCs was significantly increased (P<0.01, n=6), whereas it was significantly decreased following pre-treatment with ML133 (P<0.01, n=6; Fig. 4B).

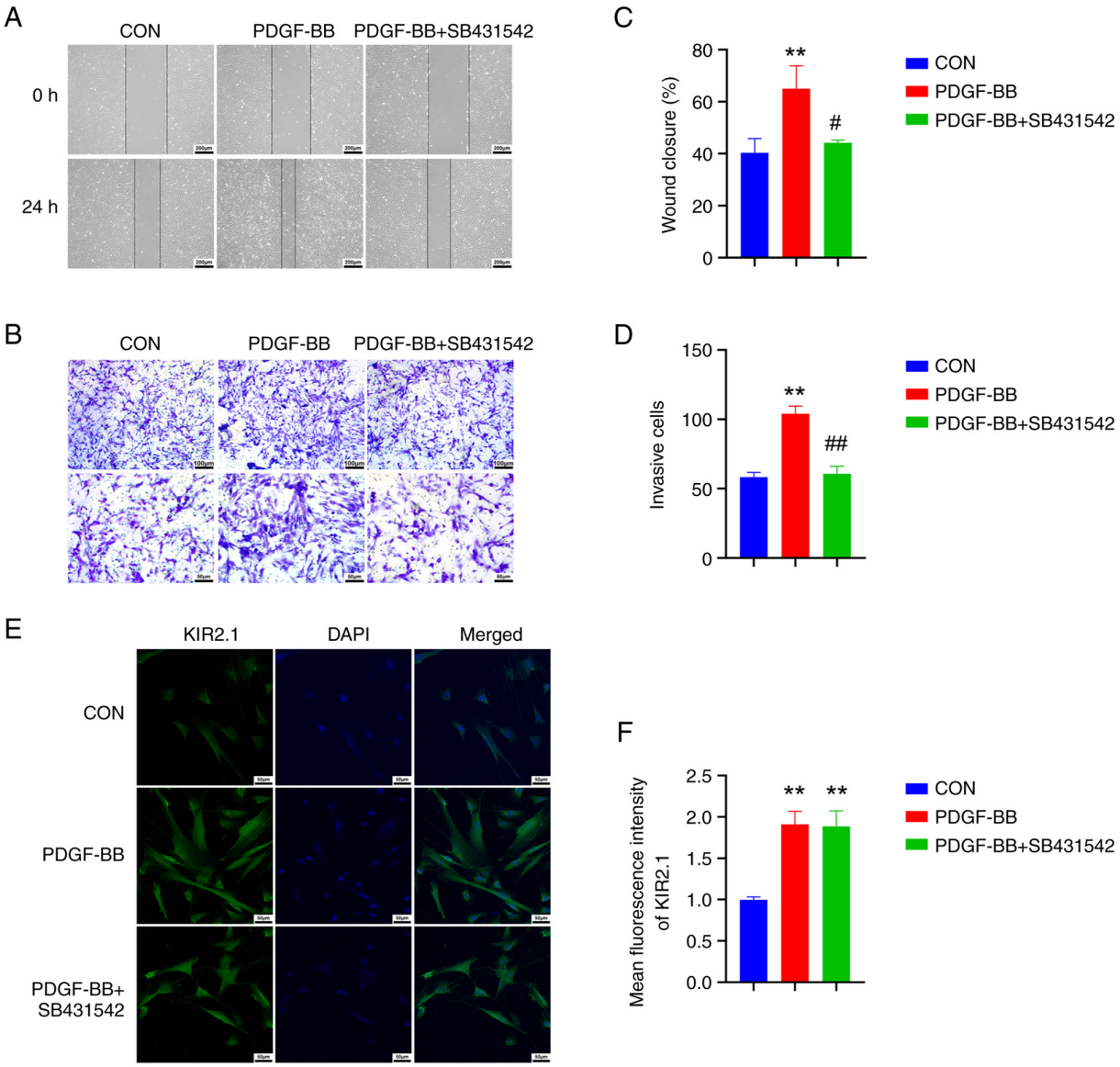

Figure 5. SB431542 reverses the proliferation and migration of human pulmonary artery smooth muscle cells induced by PDGF-BB. (A) Cell scratch images; scale bar, 200 μm. (B) Crystal violet staining results from the Transwell assay; scale bars, 100 μm (top panel) and 50 μm (bottom panel). (C) Quantitative analysis of the cell scratch healing rate. (D) Quantitative analysis of cell invasion. (E) Immunofluorescence staining for KIR2.1; scale bar, 50 μm. (F) Analysis of the relative expression of the KIR2.1 protein using immunofluorescence staining. **P<0.01, PDGF-BB vs. CON; $^{\#}$P<0.05 and $^{\#\#}$P<0.01, PDGF-BB + SB431542 vs. PDGF-BB (n=6, data were analyzed using one-way ANOVA). PDGF-BB, platelet-derived growth factor-BB; KIR2.1, inwardly rectifying K^+ channel 2.1; CON, control. PDGF-BB, platelet-derived growth factor-BB; KIR2.1, inwardly rectifying K^+ channel 2.1; CON, control.

ML133 blocks the activation of the TGF-β1/SMAD2/3 signaling pathway induced by PDGF-BB. The levels of TGF-β1/SMAD2/3 signaling pathway proteins in HPASMCs treated with PDGF-BB were examined using western blot analysis to investigate the underlying molecular mechanisms (Fig. 4A). PDGF-BB increased the levels of TGF-β1, p-SMAD2 and p-SMAD3 in HPASMCs (P<0.01 or P<0.05, n=6) and activated the TGF-β1/SMAD2/3 signaling pathway. Following pre-treatment with ML133, the levels of TGF-β1 and p-SMAD2/3 were significantly decreased (P<0.01 or P<0.05, n=6), and the TGF-β1/SMAD2/3 signaling pathway was inhibited (Fig. 4E-G).

The TGF-β1/SMAD2/3 blocker, SB431542, inhibits the proliferation and migration of HPASMCs, but does not affect KIR2.1 expression. The HPASMCs were pre-treated with the TGF-β1/SMAD2/3 inhibitor, SB431542, and the changes in cell proliferation were observed following the PDGF-BB intervention to further elucidate the role of the TGF-β1/SMAD2/3 signaling pathway in HPASMC proliferation and migration. Compared with the PDGF-BB group, the cell scratch healing level was reduced in the PDGF-BB + SB431542 group (Fig. 5A and C), and the number of cells migrating through the Transwell™ was decreased (P<0.01 or P<0.05, n=6; Fig. 5B and D), indicating that cell proliferation and migration were decreased. The expression of the OPN and PCNA proteins was examined using western blot analysis (Fig. 6A), and the results were consistent with the phenotype. Following pre-treatment with SB431542, OPN and PCNA protein expression was significantly decreased (P<0.01 or P<0.05, n=6; Fig. 6C and D).

Based on the aforementioned results, it was found that PDGF-BB upregulates KIR2.1 protein expression in

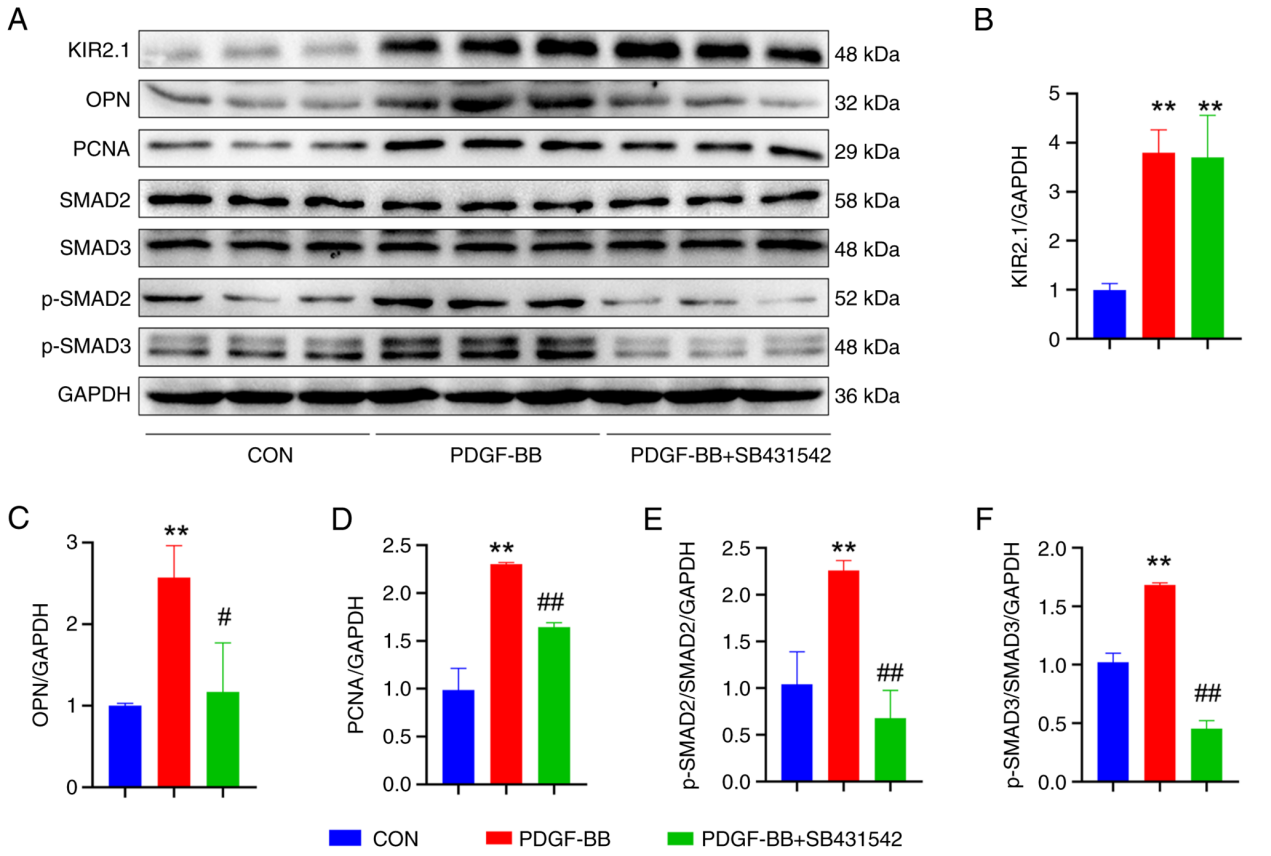

Figure 6. SB431542 alters the expression of related proteins in human pulmonary artery smooth muscle cells treated with PDGF-BB. (A) Representative western blots illustrating the levels of KIR2.1, OPN, PCNA, TGF-β1, SMAD2, SMAD3, p-SMAD2, p-SMAD3 and GAPDH. (B) Analysis of KIR2.1 levels. (C) Analysis of OPN levels. (D) Analysis of PCNA levels. (E) Analysis of p-SMAD2 and SMAD2 levels. (F) Analysis of p-SMAD3 and SMAD3 levels. **P<0.01, PDGF-BB vs. CON; $^{\#}$P<0.05 and $^{\#\#}$P<0.01, PDGF-BB + SB431542 vs. PDGF-BB (n=6, data were analyzed using one-way ANOVA). PDGF-BB, platelet-derived growth factor-BB; KIR2.1, inwardly rectifying K^+ channel 2.1; OPN, osteopontin; PCNA, proliferating cell nuclear antigen; CON, control.

HPASMCs and activates the TGF-β1/SMAD2/3 signaling pathway. The present study then further investigated the upstream and downstream association between KIR2.1 and the TGF-β1/SMAD2/3 signaling pathway by detecting changes in KIR2.1 levels following pre-treatment with SB431542. The results of immunofluorescence staining and western blot analysis (Figs. 5E and 6A) revealed that the SMAD2/3 signaling pathway was inhibited following pre-treatment with SB431542 (P<0.01 or P<0.05, n=6; Fig. 6E and F); however, no significant differences in KIR2.1 protein expression were observed between the PDGF-BB + SB431542 group and the PDGF-BB group (P>0.05, n=6; Figs. 5F and 6B).

On the whole, PDGF-BB activated the TGF-β1/SMAD2/3 signaling pathway and upregulated the expression of OPN and PCNA to promote cell proliferation and migration. ML133 inhibited KIR2.1 channel activation and modulated the downstream TGF-β1/SMAD2/3 signaling pathway. The activation of the TGF-β1/SMAD2/3 signaling pathway was blocked by SB431542; however, the expression of KIR2.1 was not affected, indicating that KIR2.1 is located upstream of the TGF-β1/SMAD2/3 signaling pathway (Fig. 7).

Discussion

The main findings of the present study were the following: Significant right ventricular remodeling and PVR were observed in the rats with PH, and obvious PVR and pulmonary fibrosis were detected. The expression of the KIR2.1, OPN and PCNA proteins in pulmonary vessels and lung tissues increased, and the TGF-β1/SMAD2/3 signaling pathway was activated. PDGF-BB upregulated the expression of the KIR2.1 protein, activated the TGF-β1/SMAD2/3 signaling pathway, and promoted the proliferation and migration of smooth muscle cells. The KIR2.1 protein inhibitor, ML133, blocked the activation of the TGF-β1/SMAD2/3 signaling pathway by PDGF-BB, and inhibited the proliferation and migration of smooth muscle cells. SB431542, an inhibitor of TGF-β1/SMAD2/3 signaling, reduced the proliferation and migration of HPASMCs induced by PDGF-BB, but did not affect KIR2.1 expression.

The main characteristics of PH are PVR and right ventricular hypertrophy (1). An intraperitoneal injection of MCT is one of the most classic methods used to establish PH models. In the present study, the MCT group exhibited a decrease in PAAT and an increase in RVHI%. In addition, the expression of the migration-related protein, OPN, and the proliferation-related protein, PCNA, was detected in pulmonary blood vessels and lung tissues. The results revealed significantly higher levels of the OPN and PCNA proteins in rats with PH than in the control group. The regulatory role of PDGF-BB in VSMC proliferation, migration and phenotype has been extensively studied (40,41). In the present study,

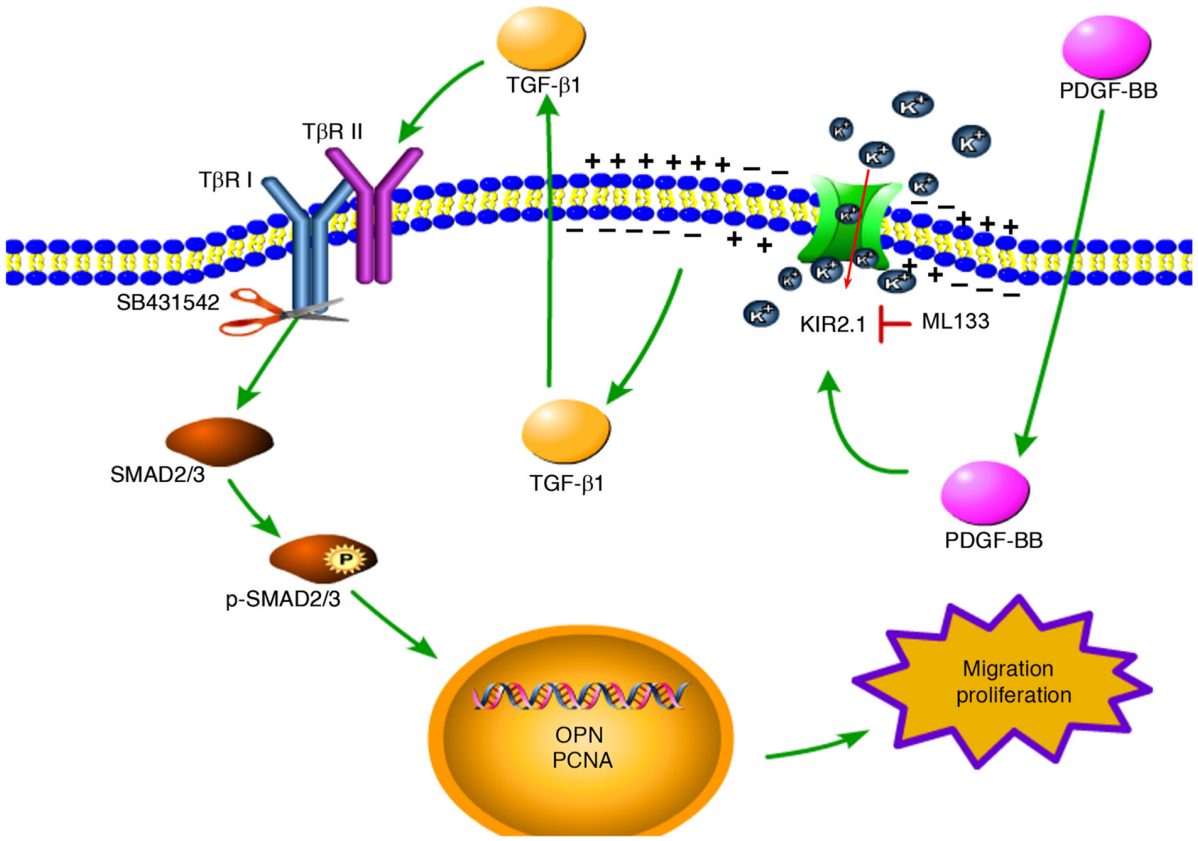

Figure 7. KIR2.1 is involved in PDGF-BB-induced cell proliferation and migration. PDGF-BB activated the TGF-β1/SMAD2/3 signaling pathway and upregulated the expression of OPN and PCNA to promote cell proliferation and migration. ML133 inhibited KIR2.1 channel activation and modulated the downstream TGF-β1/SMAD2/3 signaling pathway. The activation of the TGF-β1/SMAD2/3 signaling pathway was blocked by SB431542; however, the expression of KIR2.1 was not affected, indicating that KIR2.1 is located upstream of the TGF-β1/SMAD2/3 signaling pathway. PDGF-BB upregulated KIR2.1 protein expression, activated the KIR2.1 channel, and promoted K^+ ion influx (red arrow) and cell membrane depolarization. Subsequently, the TGF-β1/SMAD2/3 signaling pathway was activated to regulate the proliferation and migration of pulmonary artery smooth muscle cells. KIR2.1, inwardly rectifying K^+ channel 2.1; PDGF-BB, platelet-derived growth factor-BB; OPN, osteopontin; PCNA, proliferating cell nuclear antigen.

in vitro, it was found that PDGF-BB stimulation promoted HPASMC proliferation and migration, and upregulated OPN and PCNA protein expression in the cells.

K^+ channels are closely related to the proliferation and apoptosis of PASMCs (42). To date, four different types of K^+ channels have been identified in smooth muscle cells: Voltage-gated K^+ (Kv) channels (43,44), ATP-sensitive potassium (K_{ATP}) channels (45), large conductance Ca^{2+}-activated K^+ (BK Ca) channels (44,46,47) and KIR channels (22,41,48). The contribution of KIR2.1 to proliferation and migration is relatively controversial and may also be dependent on the cell type. In human heart c-kit$^+$ progenitor cells, the cell membrane potential is depolarized by silencing the KIR2.1 channel, and cell proliferation is not affected, although the cell migration rate is increased (16). In microglia, the inhibition of KIR2.1 has been found to increase cell proliferation, but to reduce cell migration (17). In rat VSMC, the knockdown of KIR2.1 expression has been shown to inhibit PDGF-BB-induced cell proliferation, migration, phenotype and intimal hyperplasia following balloon injury (22). In the human thoracic aorta, KIR2.1 has been found to be related to VSMC proliferation and vascular remodeling (18). In the present study, the protein expression of KIR2.1 was detected in pulmonary blood vessels and lung tissues, and a significantly higher protein expression of KIR2.1 was observed in pulmonary arteries and lung tissues of rats with PH than in the control group. KIR2.1 is closely related to PH development and PVR. *In vitro*, PDGF-BB promoted cell proliferation and migration, while upregulating the protein expression of KIR2.1 in cells. Following treatment with the KIR2.1 inhibitor, ML133, the proliferation and migration induced by PDGF-BB were inhibited, while the protein expression levels of OPN and PCNA were decreased. Therefore, the present study demonstrated that the KIR2.1 channel participates in PASMC proliferation and migration, as well as in PVR. The present study aimed to verify the current changes in KIR2.1 function using the whole-cell patch clamp technique. However, due to the limited HPASMC volume and small KIR2.1 current, the experimental process and results were not ideal. Therefore, the whole-cell patch clamp technique could not be used for validation experiments in the present study.

For cell proliferation, cell viability (49), apoptosis [expression of apoptosis-related genes (Bcl-2, cleaved caspase-3 and Bax)] (50) and the cell cycle (51) can further influence cell proliferation. The inhibition of KIR2.1 channel-induced depolarization has been shown to promote the biological activity and differentiation of late endothelial progenitor cells (52). Another study found that the inhibition of KIR2.1 channels increased cell mobility without affecting cell cycling progression in human cardiac c-kit$^+$ progenitor cells (16). A previous

study on BV2 microglial cells demonstrated that hypoxia induced the apoptosis of cells by upregulating KIR2.1 protein to activate mitochondria-related apoptotic pathways (50). However, such experiments have not been previously reported using PASMCs, at least to the best of our knowledge. Therefore, whether KIR2.1 channels can affect the proliferation and migration of PASMCs by regulating cell proliferation, cell viability and apoptosis warrants further investigation.

The TGF-β signaling pathway regulates various cardiovascular diseases (53). In the MCT-induced PH model, the expression of the TGF-β1 protein and the levels of p-SMAD2/3 have been shown to be significantly increased, promoting the proliferation and migration of smooth muscle cells, PVR and increasing pulmonary vascular resistance, ultimately accelerating the occurrence and development of PH (54). In the present study, *in vivo*, the levels of TGF-β1 and p-SMAD2/3 proteins in rats with PH were higher than those in the control group, and the TGF-β1/SMAD2/3 signaling pathway was activated, consistent with the findings of previous research (54). *In vitro*, PDGF-BB increased the TGF-β1 and p-SMAD2/3 protein levels in HPASMCs, and activated the TGF-β1/SMAD2/3 signaling pathway. At the same time, TGF-β1 is also an indicator of fibrosis (55). *In vivo*, the present study found that the pulmonary blood vessels and lung tissues of the rats with PH induced by MCT exhibited obvious fibrosis. TGF-β1 is closely related to a depolarized membrane potential (56). When applied for 24 to 48 h, TGF-β1 causes substantial membrane depolarization concomitant with a several-fold increase of transmembrane currents (56). In the *in vitro* experiments in the present study, following the inhibition of KIR2.1, the protein expression levels of TGF-β1 and p-SMAD2/3 were decreased, and the TGF-β1/SMAD2/3 signaling pathway was inhibited. The activation of the KIR2.1 channel promotes K^+ ion influx and cell membrane depolarization and may regulate the TGF-β1/SMAD2/3 signaling pathway to alter the proliferation and migration of HPASMCs.

In the present study, he TGF-β1/SMAD2/3 signaling pathway inhibitor, SB431542, was used to further verify the upstream and downstream relationship between KIR2.1 and the TGF-β1/SMAD2/3 signaling pathway. The blockade of the TGF-β1/SMAD2/3 signaling pathway reversed PDGF-BB-induced cell proliferation and migration, and reduced the OPN and PCNA protein levels. However, blocking the TGF-β1/SMAD2/3 signaling pathway did not affect the protein expression of KIR2.1. Therefore, KIR2.1 is located upstream of the TGF-β1/SMAD2/3 signaling pathway. PDGF-BB upregulates KIR2.1 protein expression, activates the KIR2.1 channel, promotes K^+ ion influx and cell membrane depolarization, and then activates the TGF-β1/SMAD2/3 signaling pathway to regulate PASMC proliferation and migration (Fig. 7).

In conclusion, the present study demonstrates that KIR2.1 is involved in PVR and the generation of PH, potentially as the KIR2.1 channel regulates the activity of the TGF-β1/SMAD2/3 signaling pathway by regulating cell membrane depolarization, thereby modulating the proliferation and migration of PASMCs and participating in PVR. Therefore, KIR2.1 may serve as a potential therapeutic target for the prevention or treatment of PH.

Acknowledgements

The present study was performed at the Key Laboratory of Xinjiang Endemic and Ethnic Diseases of Xinjiang Provincial Department of Physiology, Shihezi University School of Medicine.

Funding

The present study was supported by the National Natural Science Foundation of China (grant nos. 81560081 and 81960188), the Financial science and technology plan project of Xinjiang production and Construction Corps (grant no. 2020AB019) and the Research Project of Shihezi University (grant no. ZZZC201954A).

Availability of data and materials

The datasets used and/or analyzed during the current study are available from the corresponding author on reasonable request.

Authors' contributions

NC, LL and JQS conceived and designed the experiments. NC, WYS and NA conducted the experiments. RJG, WJQ, LJYK, AMZ and JRZ assisted with the experiments. NC, KTM, LL and XCT analyzed the data. NC and JQS wrote the manuscript. NC, JQS and LL revised and reviewed the manuscript. All authors discussed and commented on the manuscript and all authors have read and approved the final manuscript. NC and JQS confirm the authenticity of all the raw data.

Ethics approval and consent to participate

All procedures involving animals were performed in accordance with ethical standards and approved by the Institutional Animal Care and Use Committee of the Affiliated Hospital of Shihezi University School of Medicine (approval no. A 2020-165-01). Applicable guidelines were followed in accordance with the 'Guide for the Care and Use' published by the American Physiological Society (23).

Patient consent for publication

Not applicable.

Competing interests

The authors declare that they have no competing interests.

References

1. Crosby A, Jones F, Kolosionek E, Southwood M, Purvis I, Soon E, Butrous G, Dunne DE and Morrell NW: Praziquantel reverses pulmonary hypertension and vascular remodeling in murine schistosomiasis. Am J Respir Crit Care Med 184: 467-473, 2011.
2. Pabani S and Mousa S: Current and future treatment of pulmonary hypertension. Drugs Today (Barc) 48: 133-147, 2012.
3. Kim G, Ryan J, Marsboom G and Archer SL: Epigenetic mechanisms of pulmonary hypertension. Pulm Circ 1: 347-356, 2011.

4. Schermuly RT, Ghofrani HA, Wilkins MR and Grimminger F: Mechanisms of disease: Pulmonary arterial hypertension. Nat Rev Cardiol 8: 443-455, 2011.
5. Schermuly RT, Dony E, Ghofrani HA, Pullamsetti S, Savai R, Roth M, Sydykov A, Lai YJ, Weissmann N, Seeger W and Grimminger F: Reversal of experimental pulmonary hypertension by PDGF inhibition. J Clin Invest 115: 2811-2821, 2005.
6. Klein M, Schermuly RT, Ellinghaus P, Milting H, Riedl B, Nikolova S, Pullamsetti SS, Weissmann N, Dony E, Savai R, *et al*: Combined tyrosine and serine/threonine kinase inhibition by sorafenib prevents progression of experimental pulmonary hypertension and myocardial remodeling. Circulation 118: 2081-2090, 2008.
7. Yue Y, Li YQ, Fu S, Wu YT, Zhu L, Hua L, Lv JY, Li YL and Yang DL: Osthole inhibits cell proliferation by regulating the TGF-β1/Smad/p38 signaling pathways in pulmonary arterial smooth muscle cells. Biomed Pharmacother 121: 109640, 2020.
8. Wang XB, Wang W, Zhu XC, Ye WJ, Cai H, Wu PL, Huang XY and Wang LX: The potential of asiaticoside for TGF-β1/Smad signaling inhibition in prevention and progression of hypoxia-induced pulmonary hypertension. Life Sci 137: 56-64, 2015.
9. Yu W, Liu D, Liang C, Ochs T, Chen S, Chen S, Du S, Tang C, Huang Y, Du J and Jin H: Sulfur dioxide protects against collagen accumulation in pulmonary artery in association with downregulation of the transforming growth factor β1/smad pathway in pulmonary hypertensive rats. J Am Heart Assoc 5: e003910, 2016.
10. Ma W, Han W, Greer PA, Tuder RM, Toque HA, Wang KKW, Caldwell RW and Su Y: Calpain mediates pulmonary vascular remodeling in rodent models of pulmonary hypertension, and its inhibition attenuates pathologic features of disease J Clin Invest 121: 4548-4566, 2011.
11. Thomas M, Docx C, Holmes AM, Beach S, Duggan N, England K, Leblanc C, Lebret C, Schindler F, Raza F, *et al*: Activin-like kinase 5 (ALK5) mediates abnormal proliferation of vascular smooth muscle cells from patients with familial pulmonary arterial hypertension and is involved in the progression of experimental pulmonary arterial hypertension induced by monocrotaline. Am J Pathol 174: 380-389, 2009.
12. Hibino H, Inanobe A, Furutani K, Murakami S, Findlay I and Kurachi Y: Inwardly rectifying potassium channels: Their structure, function, and physiological roles. Physiol Rev 90: 291-366, 2010.
13. Wu L, Wang Q, Gu J, Zhang H and Gu Y: Modulation of actin filament dynamics by inward rectifying of potassium channel Kir2.1. Int J Mol Sci 21: 7479, 2020.
14. Ji CD, Wang YX, Xiang DF, Liu Q, Zhou ZH, Qian F, Yang L, Ren Y, Cui W, Xu SL, *et al*: Kir2.1 interaction with Stk38 promotes invasion and metastasis of human gastric cancer by enhancing MEKK2-MEK1/2-ERK1/2 signaling. Cancer Res 78: 3041-3053, 2018.
15. Anton R, Ghenghea M, Ristoiu V, Gattlen C, Suter MR, Cojocaru PA, Popa-Wagner A, Catalin B and Deftu AF: Potassium channels Kv1.3 and Kir2.1 but not Kv1.5 contribute to BV2 cell line and primary microglial migration. Int J Mol Sci 22: 2081, 2021.
16. Zhang Y, Li G, Che H, Sun HY, Xiao GS, Wang Y and Li GR: Effects of BKCa and Kir2.1 channels on cell cycling progression and migration in human cardiac c-kit+ progenitor cells. PLoS One 10: e0138581, 2015.
17. Lam D and Schlichter L: Expression and contributions of the Kir2.1 inward-rectifier K(+) channel to proliferation, migration and chemotaxis of microglia in unstimulated and anti-inflammatory states. Front Cell Neurosci 9: 185, 2015.
18. Karkanis T, Li S, Pickering JG and Sims SM: Plasticity of KIR channels in human smooth muscle cells from internal thoracic artery. Am J Physiol Heart Circ Physiol 284: H2325-H2334, 2003.
19. Bradley K, Jaggar J, Bonev A, Heppner TJ, Flynn ER, Nelson MT and Horowitz B: Kir2.1 encodes the inward rectifier potassium channel in rat arterial smooth muscle cells J Physio 515 (Pt 3): 639-651, 1999.
20. Chilton L, Loutzenhiser K, Morales E, Breaks J, Kargacin G and Loutzenhiser R: Inward rectifier K(+) currents and Kir2.1 expression in renal afferent and efferent arterioles. J Am Soc Nephrol 19: 69-76, 2008.
21. Tennant B, Cui Y, Tinker A and Clapp L: Functional expression of inward rectifier potassium channels in cultured human pulmonary smooth muscle cells: Evidence for a major role of Kir2.4 subunits J Membr Biol 213: 19-29, 2006.
22. Qiao Y, Tang C, Wang Q, Wang D, Yan G and Zhu B: Kir2.1 regulates rat smooth muscle cell proliferation, migration, and post-injury carotid neointimal formation. Biochem Biophys Res Commun 477: 774-780, 2016.
23. Bayne K: Revised guide for the care and use of laboratory animals available. American physiological society. Physiologist 39: 208-111, 1996.
24. Barman S, Li X, Haigh S, Kondrikov D, Mahboubi K, Bordan Z, Stepp DW, Zhou J, Wang Y, Weintraub DS, *et al*: Galectin-3 is expressed in vascular smooth muscle cells and promotes pulmonary hypertension through changes in proliferation, apoptosis, and fibrosis. Am J Physiol Lung Cell Mol Physiol 316: L784-L797, 2019.
25. Tian L, Wu D, Dasgupta A, Chen KH, Mewburn J, Potus F, Lima PDA, Hong Z, Zhao YY, Hindmarch CCT, *et al*: Epigenetic metabolic reprogramming of right ventricular fibroblasts in pulmonary arterial hypertension: A pyruvate dehydrogenase kinase-dependent shift in mitochondrial metabolism promotes right ventricular fibrosis. Circ Res 126: 1723-1745, 2020.
26. Zhang L, Fan Z, Wang L, Liu LQ, Li XZ, Li L, Si JQ and Ma KT: Carbenoxolone decreases monocrotaline-induced pulmonary inflammation and pulmonary arteriolar remodeling in rats by decreasing the expression of connexins in T lymphocytes. Int J Mol Med 45: 81-92, 2020.
27. Flues K, Moraes-Silva I, Mostarda C, Souza PRM, Diniz GP, Moreira ED, Piratello AC, Chaves MLB, Angelis KD, Salemi VMC, *et al*: Cardiac and pulmonary arterial remodeling after sinoaortic denervation in normotensive rats. Auton Neurosci 166: 47-53, 2012.
28. Yared K, Noseworthy P, Weyman AE, McCabe E, Picard MH and Baggish AL: Pulmonary artery acceleration time provides an accurate estimate of systolic pulmonary arterial pressure during transthoracic echocardiography. J Am Soc Echocardiogr 24: 687-692, 2011.
29. Wang L, Zhang F, Li J, Liu Z, Kou Y, Song Y, Xu H, Wang H and Wang Y: Using pulmonary artery acceleration time to evaluate pulmonary hemodynamic changes on preterm infants with respiratory distress syndrome. Transl Pediatr 10: 2287-2297, 2021.
30. Zaky A, Zafar I, Masjoan-Juncos JX, Husain M, Mariappan N, Morgan CJ, Hamid T, Frölich MA, Ahmad S and Ahmad A: Echocardiographic, biochemical, and electrocardiographic correlates associated with progressive pulmonary arterial hypertension. Front Cardiovasc Med 8: 705666, 2021.
31. Yang J, Zhou R, Zhang M, Tan HR and Yu JQ: Betaine attenuates monocrotaline-induced pulmonary arterial hypertension in rats via inhibiting inflammatory response. Molecules 23: 1274, 2018.
32. Zhang LZ, Fan ZR, Wang L, Liu LQ, Li XZ, Li L, Si JQ and Ma KT: Carbenoxolone decreases monocrotaline-induced pulmonary inflammation and pulmonary arteriolar remodeling in rats by decreasing the expression of connexins in T lymphocytes. Int J Mol Med 45: 81-92, 2020.
33. Baldwin SN, Sandow SL, Mondéjar-Parreño G, Stott JB and Greenwood IA: K(V)7 channel expression and function within rat mesenteric endothelial cells. Front Physiol 11: 598779, 2020.
34. Ji Z, Li J and Wang J: Jujuboside b inhibits neointimal hyperplasia and prevents vascular smooth muscle cell dedifferentiation, proliferation, and migration via activation of AMPK/PPAR-γ signaling. Front Pharmacol 12: 672150, 2021.
35. Zuo W, Liu N, Zeng Y, Xiao Z, Wu K, Yang F, Li B, Song Q, Xiao Y and Liu Q: Luteolin ameliorates experimental pulmonary arterial hypertension via suppressing hippo-YAP/PI3K/AKT signaling pathway. Front Pharmacol 12: 663551-663551, 2021.
36. Niu W, Lim TC, Alshihri A, Rajappa R, Wang L, Kurisawa M and Spector M: Platelet-derived growth factor stimulated migration of bone marrow mesenchymal stem cells into an injectable gelatin-hydroxyphenyl propionic acid matrix. Biomedicines 9: 203, 2021.
37. An Z, Liu Y, Song ZS, Tang H, Yuan Y and Xu ZY: Mechanisms of aortic dissection smooth muscle cell phenotype switch. J Thorac Cardiovasc Surg 154: 1511-1521.e6, 2017.
38. Song W, Li L, Jia Q, Cao N, Li L, Ma K and Si J: Monocrotaline pyrrole induces A549 cells and activates TGF-β1/SMAD2/SMAD3 pathway to promote proliferation and migration of human pulmonary artery smooth muscle cells. Xi Bao Yu Fen Zi Mian Yi Xue Za Zhi 36: 527-534, 2020 (In Chinese).
39. Jia Q, Li L, Song W, Cao N, Li L, Ma K and Si J: Up-regulation of connexin 43 (Cx43) by angiotensin II promotes the proliferation and migration of human pulmonary artery smooth muscle cells. Xi Bao Yu Fen Zi Mian Yi Xue Za 36: 616-621, 2020 (In Chinese).
40. Raines EW: PDGF and cardiovascular disease. Cytokine Growth Factor Rev 15: 237-254, 2004.

41. Tang C, Wang D, Luo E, Yan G, Liu B and Hou J: Activation of inward rectifier K(+) channel 2.1 by PDGF-BB in rat vascular smooth muscle cells through protein kinase a. Biomed Res Int 1: 4370832, 2020.
42. Burg ED, Remillard CV and Yuan JXJ: Potassium channels in the regulation of pulmonary artery smooth muscle cell proliferation and apoptosis: Pharmacotherapeutic implications. Br J Pharmacol 153: S99-S111, 2008.
43. Mondejar-Parreño G, Perez-Vizcaino F and Cogolludo A: Kv7 channels in lung diseases. Front Physiol 11: 634, 2020.
44. Iqbal H, Verma AK, Yadav P, Alam S, Shafiq M, Mishra D, Khan F, Hanif K, Negi AS and Chanda D: Antihypertensive effect of a novel angiotensin II receptor blocker fluorophenyl benzimidazole: Contribution of cGMP, voltage-dependent calcium channels, and BK channels to vasorelaxant mechanisms. Front Pharmacol 12: 611109, 2021.
45. Jin X, Wu Y, Cui N, Jiang C and Li SS: Methylglyoxal-induced miR-223 suppresses rat vascular K channel activity by downregulating Kir6.1 mRNA in carbonyl stress. Vascula Pharmacol 128-129: 106666, 2020.
46. Shen X, Zhang L, Jiang L, Xiong W, Tang Y, Lin L and Yu T: Alteration of sphingosine-1-phosphate with aging induces contractile dysfunction of colonic smooth muscle cells via Ca^{2+}-activated K channel (BK_{Ca}) upregulation. Neurogastroenterol Motil 33: e14052, 2021.
47. Li Y, Bai J, Yang YH, Hoshi N and Chen DB: Hydrogen sulfide relaxes human uterine artery via activating smooth muscle BK_{Ca} channels. Antioxidants (Basel) 9: 1127, 2020.
48. Yuan XJ: Voltage-gated K+ currents regulate resting membrane potential and [Ca2+]i in pulmonary arterial myocytes. Circ Res 77: 370-378, 1995.
49. Wang H, Zhang W, Gao Q, Cao X, Li Y, Li X, Min Z, Yu Y, Guo Y and Shuai L: Extractive from hypericum ascyron L promotes serotonergic neuronal differentiation in vitro. Stem Cell Res 31: 42-50, 2018.
50. Xie YF, Wang Y, Rong Y, He W, Yan M, Li X, Si J, Li L, Zhang Y and Ma K: Hypoxia induces apoptosis of microglia BV2 by upregulating Kir2.1 to activate mitochondrial-related apoptotic pathways. Dis Markers 17: 5855889, 2022.
51. Gao Q, Zhang W, Zhao Y, Tian Y, Wang Y, Zhang J, Geng M, Xu M, Yao C, Wang H, *et al*: High-throughput screening in postimplantation haploid epiblast stem cells reveals Hs3st3b1 as a modulator for reprogramming. Stem Cells Transl Med 10: 743-755, 2021.
52. Zhang X, Cui X, Li X, Yan H, Li H, Guan X, Wang Y, Liu S, Qin X and Cheng M: Inhibition of Kir2.1 channel-induced depolarization promotes cell biological activity and differentiation by modulating autophagy in late endothelial progenitor cells. J Mol Cell Cardiol 127: 57-66, 2019.
53. Goumans M and Dijke PT: TGF-β signaling in control of cardiovascular function. Cold Spring Harbor Perspect Biol 10: a022210, 2018.
54. Cao N, Tang X, Gao R, Kong L, Zhang J, Qin W, Hu N, Zhang A, Ma K, Li L and Si JQ: Galectin-3 participates in PASMC migration and proliferation by interacting with TGF-β1. Life Sci 1274: 119347, 2021.
55. Meng XM, Nikolic-Paterson DJ and Lan HY: TGF-β: The master regulator of fibrosis. Nat Rev Nephrol 12: 325-338, 2016.
56. Salvarani N, Maguy A, De Simone S, Miragoli M, Jousset F and Rohr S: TGF-β_1 (Transforming Growth Factor-β_1) plays a pivotal role in cardiac myofibroblast arrhythmogenicity. Cir Arrhythm Electrophysiol 10: e004567, 2017.